FEBS Letters 585 (2011) 545–548

FEBS Letters
journal homepage: www.FEBSLetters.org

# Axial ligation of the high-potential heme center in an *Arabidopsis* cytochrome *b*561

Filip Desmet [a], Alajos Bérczi [b], László Zimányi [b], Han Asard [c], Sabine Van Doorslaer [a,*]

[a] Department of Physics, University of Antwerp, Belgium
[b] Institute of Biophysics, Biological Research Center of the Hungarian Academy of Sciences, Szeged, Hungary
[c] Department of Biology, University of Antwerp, Belgium

ARTICLE INFO

*Article history:*
Received 29 October 2010
Revised 21 December 2010
Accepted 4 January 2011
Available online 12 January 2011

Edited by Miguel De la Rosa

*Keywords:*
Double mutant
EPR
Cytochrome b561
Optical absorption spectroscopy
Resonance Raman spectroscopy

ABSTRACT

***Arabidopsis* has four putative, di-heme cytochrome *b*561 proteins, including one localized in the tonoplast (TCytb). From a comparative electron paramagnetic resonance (EPR), UV–Vis absorption and resonance Raman study, on wild type, H83A/H156A-TCytb and H83L/H156L-TCytb double mutants, it follows that the H83 and H156 residues are binding one of the two hemes. These measurements show that the high-potential heme site is situated at the cytoplasmic side of the membrane and allow the unambiguous differentiation between two models on the heme localization in cytochrome *b*561 proteins.**


## 1. Introduction

Cytochromes b561 (Cyts-b561) are ascorbate (ASC)-reducible, *trans*-membrane, di-heme proteins identified in a great variety of organisms, including invertebrates, vertebrates and plants [1]. All Cyts-b561 are predicted to consist of six *trans*-membrane helices, with four highly conserved His residues likely involved in the heme coordination [2]. *Arabidopsis* and other plants contain several genes encoding putative Cyts-b561; however, little is known about the localization and physiological function of the gene products [3]. One plant isoform is localized on the tonoplast and is named tonoplast-Cyt-b561 (TCytb or TCB). Cyts-b561 are generally accepted to catalyze ASC-driven *trans*-membrane electron transport. This activity has been demonstrated for TCytb by expression in yeast cells and measuring ASC-dependent reduction of extracellular ferric-chelates [4].

The chromaffin granule cytochrome b561 (CGCytb) is the most studied member of this protein family [5–11]. The oxidized CGCytb was investigated using electron paramagnetic resonance (EPR) spectroscopy, showing that the two heme centers have distinct EPR signatures [9–11]. Both centers have EPR spectra typical of low-spin ferric heme centers, with characteristic signals at $g_z = 3.7$, and $g_z = 3.1$, for the low and high-potential heme. Combining EPR and site-directed mutagenesis for CGCytb, the heme ligands were identified as His54 and His122 at the matrix (intravesicular) side (M-side) for the low-potential heme, while His88 and His161, located at the cytoplasmic (extravesicular) side (C-side), ligate the high-potential heme [11]. Furthermore, mutation of the His92 residue, situated near the C-side heme in CGCytb561, caused a shift in the position of the $g_z = 3.1$ signal, whereas mutation of His110, in the vicinity of the M-side heme, induced a change in the $g_z = 3.7$ signal [12].

In this work, we use a combination of EPR, UV–Vis absorption and resonance Raman (RR) spectroscopy with site-directed mutagenesis, to investigate the heme ligation of TCytb in *Arabidopsis*. The results will be compared to those of other Cyt-b561 proteins, such as CGCytb and the recently characterized putative tumor suppressor 101F6 protein (TSCytb) [13].

## 2. Materials and methods

### 2.1. Materials

Yeast cell growth, microsomal membrane preparation, and protein purification by His-tag affinity chromatography were performed as described [3,4]. H83A/H156A-TCytb and H83L/H156L-TCytb were obtained by site-directed mutagenesis using the

*Abbreviations:* ASC, ascorbate; Cyt-*b*561, cytochrome b561; TCytb or TCB, tonoplast-Cyt-b561; CGCytb, chromaffin granule cytochrome b561; EPR, electron paramagnetic resonance; TSCytb, tumor suppressor 101F6 protein; RR, resonance Raman

* Corresponding author. Address: Department of Physics, University of Antwerp, Campus Drie Eiken, Universiteitsplein 1, 2610 Wilrijk, Belgium. Fax: +32 32652470.
*E-mail address:* sabine.vandoorslaer@ua.ac.be (S. Van Doorslaer).

0014-5793/$36.00 
doi:10.1016/j.febslet.2011.01.006

QuickChange mutagenesis kit (Stratagene, La Jolla, CA, USA) [14,15]. All sequences were confirmed by DNA sequencing.

Proteins were solubilized in potassium phosphate buffer, pH 7 (50 mM $KH_2PO_4$, pH adjusted with NaOH), containing 150 mM NaCl, 10% (w/v) glycerol and 0.5 mM dodecyl-β-D-maltoside. This buffer was used in all spectroscopy studies. The purified protein is in the ferric (oxidized) form.

### 2.2. Absorption spectroscopy

Absorption spectra were recorded in split beam mode between 500 and 600 nm on an OLIS-updated SLM-Aminco DW2000 spectrophotometer (Bogart GA, USA) with 2 nm slit-width and 0.5 nm $s^{-1}$ scan rate at 77 K. Data analysis and curve fitting were performed using the SPSERV and Origin8.0 software.

### 2.3. Redox titration

Redox titration was performed under argon atmosphere in the presence of redox mediators at room temperature [15]. Data analysis is based on [16] (Supplementary data).

### 2.4. Resonance Raman spectroscopy

RR measurements were carried out on a Dilor XY-800 Raman scattering spectrometer (Lille, France) consisting of a triple 800 nm spectrograph, operating in low-dispersion mode with CCD detection. The spectra were corrected for the RR background of the used buffer. Protein concentrations for RR experiments were ~0.5 mg/ml. Protein reduction was achieved with 20 mM ASC.

### 2.5. EPR spectroscopy

The X-band (microwave frequency of 9.43 GHz) continuous-wave EPR spectra were recorded on a Bruker ESP300E spectrometer (Rheinstetten, Germany) equipped with a gas-flow cryogenic system (Oxford Inc., Oxford, UK). The magnetic field was measured with a Bruker ER035M NMR Gaussmeter. EPR spectra were recorded with a modulation amplitude of 0.5 mT, a microwave power of 5 mW and modulation frequency of 100 kHz. During the experiments, the EPR tubes were attached to a vacuum line in order to remove paramagnetic $O_2$. The EPR spectra were simulated using EasySpin [17]. Typical protein concentrations were 2–5 mg/ml.

## 3. Results and discussion

The two pairs of His residues coordinating the two hemes in TCytb have distinct roles in obtaining a functional recombinant protein. When His50 or His117 were mutated to Ala, no functional protein was obtained, while mutation of His83 or His156 yielded functional recombinant proteins [14]. We focus here on the H83A/H156A and the H83L/H156L double mutants of His-tagged TCytb to: (1) test how the absence of the C-side heme influences the M-side heme; (2) investigate whether a bulky Leu side chain at positions 83 and 156 has a different effect than the smaller Ala replacements; (3) evaluate which of the models proposed for the localizations of the low- and high-potential hemes in Cyt-b561 proteins is valid [11,18].

The anaerobic redox titration of TCytb and its two double mutants shows that the high-potential heme is missing in the double mutants (Supplementary data). Mathematical analysis reveals that TCytb has two one-electron redox centers with midpoint redox potentials of +20 mV and +178 mV (±15 mV), while the double mutants have only one one-electron redox centre with +46 ± 11 mV (H83A/H156A-TCytb) and +21 ± 5 mV (H83L/H156L-TCytb). The former values are in agreement with those published earlier for the partially purified and untagged TCytb [4].

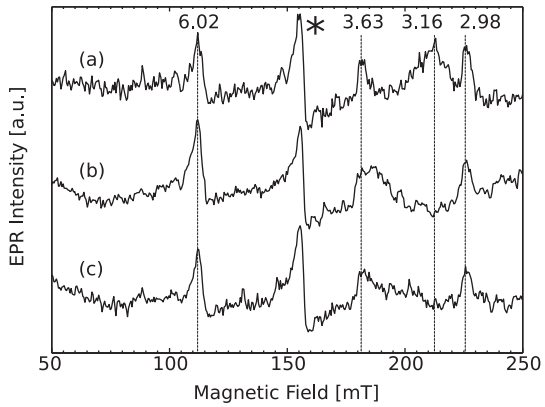


**Fig. 1.** Low-field part of EPR spectra of frozen solutions of oxidized TCytb (a), H83A/H156A TCytb (b) and H83L/H156L TCytb (c) at pH 7 and 15 K. * = signal from non-heme iron.

The EPR spectrum of oxidized partially purified and untagged TCytb displayed two distinct peaks with $g_z$ values around 3.7 and 3.1 [4]. These signals are still present in the spectra of the His-tagged and highly purified TCytb (Fig. 1a, full EPR spectrum in Supplementary data). These signals are also found for other (putative) Cytb561 proteins [9–13] and correspond to the low-field parts ($g = g_z$) of the EPR signals of the two heme centers. The signal at $g \approx 4.3$ (asterisk in Fig. 1a) is typical of extra-heme iron and is readily observed in biological samples [9–13]. The signal at $g = 6.05$ stems from a high-spin ferric iron form related to protein degradation [4,9–13]. Because of the spin-quantum-number-dependence of the EPR intensity, this signal corresponds to a minority species. In some batches, also a signal at $g_z = 2.975$ is observed (Fig. 1a). A similar feature has been observed as a minority species in other Cyt-b561 protein preparations [4,8,13]. It was also observed in CGCytb mutants where it was suggested to originate from a relaxation of the high-potential heme site [11]. Because of the batch-dependence of this signal, we ascribe this signal to protein degradation and/or misfolding.

Fig. 1b and c shows the low-field part of the EPR spectra of oxidized H83A/H156A-TCytb and H83L/H156L-TCytb, respectively. In both cases, the $g_z = 3.16$ signal has disappeared (compare to Fig. 1a), while the other EPR features remained. This corroborates the redox results that the His83/His156 couple is heme-binding. At the same time, a significant broadening of the $g_z = 3.69$ signal is observed in the EPR spectrum of H83A/H156A-TCytb (Fig. 1b). This could indicate a change in the M-side heme environment induced by the removal of the C-side heme. The redox potential found for this mutant also differs somewhat from the one obtained for H83L/H156L-TCytb and the low-potential heme of TCytb. The $g = 2.975$ signal is still present in the double mutants, excluding the earlier suggestion that this signal is due to a relaxed conformation of the C-side heme [11].

In the optical absorption spectrum of reduced TCytb taken at 77 K, a split α band (or $Q_0$ band) is readily recognized (Supplementary data). Fig. 2 shows the normalized reduced-minus-oxidized difference absorption spectra for TCytb, H83A/H156A-TCytb and H83L/H156L-TCytb for reduction with 20 mM ASC (Fig. 2A) and 2 mM dithionite (Fig. 2B). A clear change is observed in the spectra upon removal of the C-side heme. The separation between the two $Q_0$ peaks in the spectrum of ASC-reduced TCytb is significantly larger (6.4 nm) than in the case of the double mutants (6.1 nm) (Supplementary data). The fact that a split $Q_0$ band is still observed in

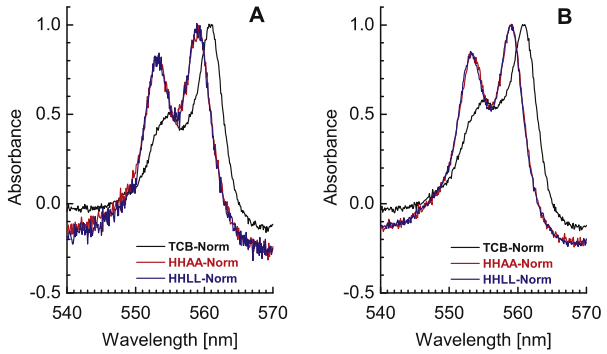


**Fig. 2.** Comparison between reduced-minus-oxidized normalized optical spectra, obtained at 77 K for TCytb (TCB-Norm), H83A/H156A TCytb (HHAA-Norm) and H83L/H156L TCytb (HHLL-Norm); (A) 20 mM ASC-reduced, (B) 2 mM dithionite-reduced. Protein concentration: ~0.5 mg/ml.

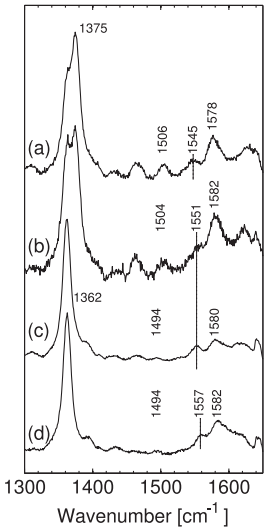


**Fig. 3.** High-frequency region of the resonance Raman spectrum of (a) oxidized TCytb, (b) oxidized H83A/H156A TCytb, (c) ASC-reduced TCytb, (d) ASC-reduced H83A/H156A TCytb.

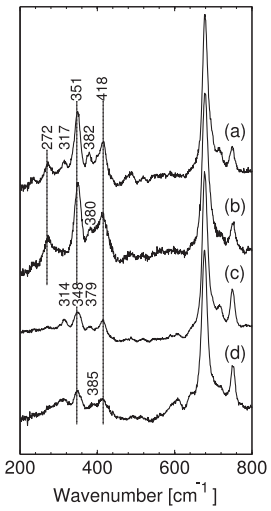


**Fig. 4.** Low-frequency region of the resonance Raman spectrum of (a) oxidized TCytb, (b) oxidized H83A/H156A TCytb, (c) ASC-reduced TCytb, (d) ASC-reduced H83A/H156A TCytb.

the mutants proves, that the splitting does not originate from the presence of two heme sites [13]. The $Q_0$ peaks of the reduced TCytb double mutants have shifted to lower wavelength (higher energy) values, compared to those in the wild-type (Fig. 2).

Figs. 3 and 4 show the high- and low-frequency range of the RR spectra of TCytb and the H83A/H156A double mutant; oxidized (Figs. 3a,b; 4a,b) and ASC-reduced (Figs. 3c,d; 4c,d). The RR spectra of the H83L/H156L mutant (not shown) are identical to those of the H83A/H156A mutant. The high-frequency region of the RR spectra contains a number of marker bands sensitive to the oxidation, spin state and coordination of the heme iron [19]. Here, we follow the assignment of the RR bands in ferric heme proteins of Hu et al. [20]. Ferric TCytb exhibits two $\nu_4$-bands at 1362 $cm^{-1}$ and 1375 $cm^{-1}$, respectively (Fig. 3a). While the latter is expected for the ferric state, the former is characteristic for a ferrous heme. This indicates that photoreduction has occurred, as supported by the laser-power dependence (Supplementary data). A similar behavior is found for ferric H83A/H156A-TCytb (Fig. 3b) and has been observed for recombinant TSCytb [13]. The $\nu_3$ bands at 1506 $cm^{-1}$ (ferric TCytb, Fig. 3a) and 1504 $cm^{-1}$ (ferric H83A/H156A-TCytb, Fig. 3b) are characteristic for a low-spin ferric state of the hemes, consistent with the bis-His coordination of the iron. Similarly, the $\nu_4/\nu_3$ pair at 1362 $cm^{-1}$/1494 $cm^{-1}$, observed in the RR spectra of ASC-reduced TCytb and H83A/H156A-TCytb (Fig. 3c and d) is characteristic for a low-spin ferrous state of the hemes. Since the $\nu_3$ and $\nu_4$ bands depend on the iron oxidation and spin state, they are not affected by the local differences between the M- and C-side heme region, and hence no splitting is observed in these bands. Although the RR spectra of the three proteins are similar, small differences can be observed in the low-frequency range (Fig. 4a and b). We observe a reduction of the signal at 317 $cm^{-1}$ and only one of the propionate $\delta(C_\beta C_c C_d)$ bending modes at 377 and 382 $cm^{-1}$ remains in the double mutant. The higher the frequency of these modes, the stronger the hydrogen bonds are between the propionate group and the surrounding amino-acid residues. The propionates of the remaining M-side heme group in the double mutant are thus more strongly hydrogen-bonded to the protein matrix than in the C-side heme. Furthermore, a small shift to higher wave numbers occurs for the signals in the 1500–1600 $cm^{-1}$ range. This shift is even more pronounced in the RR spectra of the ASC-reduced TCytb and H83A/H156A-Cytb (Fig. 3c and d). In this region we find the marker bands for the heme-core size [21]. A significant shift upon mutation is observed for the $\nu_{38}$ band from 1545 $cm^{-1}$ to 1551 $cm^{-1}$ for the ferric case (Fig. 3a and b) and from 1551 $cm^{-1}$ to 1557 $cm^{-1}$ in the ferrous case (Fig. 3c and d), but also the position of the $\nu_2$ band around 1580 $cm^{-1}$ changes after mutation. A shift to higher wave number is indicative of a smaller heme core (i.e., reduced porphyrin-center-to-porphyrin-nitrogen distance), indicating that the M-side heme shows a stronger heme deformation than the C-side heme. Both $\nu_{38}$ and $\nu_8$ bands of ferric and ferrous TCytb are broad, because they consist of the sum of the respective bands of the M- and C-side hemes.

Two models have been proposed for the localization of the two hemes in CGCytb561 and by extension all members of the Cytb561 protein family. According to the first model [18], the high-potential heme with $g_z$ = 3.13 is located on the intravesicular (M)-side of the chromaffin granule membrane and is coordinated by His54 and His122. In the second model [11], this heme is located on the C-side of the membrane and is coordinated by His88 and His161. In the *Arabidopsis* TCytb, the high-potential heme-coordinating His residues are His83 and His156 on the C-side, supporting the second model [11].

While the $g_z$ values of the two hemes in TCytb are comparable to those reported for CGCytb561 ($g_z$ = 3.7 and 3.13) [11], the one of the high-potential heme of tumor suppressor TSCytb is considerably lower (2.96) [13], pointing to an altered heme environment.

The related redox potential is also lower (141 mV (±9 mV) [13]) than for TCytb (+178 mV (±15 mV)). It is unclear at the moment why TSCytb differs from TCytb and CGCytb561 and what the function-related implications are.

## Acknowledgements

The authors thank Dr. Balázs Szalontai and Dr. Csaba Bagyinka (Institute of Biophysics, BRC, Szeged, Hungary) for their help in the UV-Vis spectrum analysis. This work was supported by the Hercules Foundation, Flanders (contract AUHA013) (to S.V.D.), and the Flemish Fund for Scientific Research, FWO (grant G.0118.07N to H.A). F.D. thanks the BOF-UA-TOP fund for PhD funding.

## Appendix A. Supplementary data

Supplementary data associated with this article can be found, in the online version, at doi:10.1016/j.febslet.2011.01.006.

## References

[1] Tsubaki, M., Takeuchi, F. and Nakanishi, N. (2005) Cytochrome *b*561 protein family: expanding roles and versatile transmembrane electron transfer abilities as predicted by a new classification system and protein sequence motif analyses. Biochim. Biophys. Acta 1763, 174–200.
[2] Okuyama, E., Yamamoto, R., Ichikawa, Y. and Tsubaki, M. (1998) Structural basis for the electron transfer across the chromaffin vesicle membranes catalyzed by cytochrome $b_{561}$: analysis of cDNA nucleotide sequences and visible absorption spectra. Biochim. Biophys. Acta 1383, 269–278.
[3] Griesen, D., Su, D., Bérczi, A. and Asard, H. (2004) Localization of an ascorbate-reducible cytochrome b561 in the plant tonoplast. Plant Physiol. 134, 726–734.
[4] Bérczi, A., Su, D. and Asard, H. (2007) An Arabidopsis cytochrome b561 with trans-membrane ferrireductase capability. FEBS Lett. 581, 1505–1508.
[5] Flatmark, T. and Terland, O. (1971) Cytochrome b561 of the bovine adrenal chromaffin granules. A high potential b-type cytochrome. Biochim. Biophys. Acta 253, 487–491.
[6] Flatmark, T. and Grønberg, M. (1981) Cytochrome b-561 of the bovine adrenal chromaffin granules. Molecular weight and hydrodynamic properties in micellar solutions of Triton X-100. Biochem. Biophys. Res. Commun. 99, 292–301.
[7] Takeuchi, F., Kobayashi, K., Tagawa, S. and Tsubaki, M. (2001) Ascorbate inhibits the carbethoxylation of two histidyl and one tyrosyl residues indispensable for the trans-membrane electron transfer reaction of cytochrome b561. Biochemistry 40, 4067–4076.
[8] Tsubaki, M., Nakayama, M., Okuyama, E., Ichikawa, Y. and Hori, H. (1997) Existence of two heme B centers in cytochrome b561 from bovine adrenal chromaffin vesicles as revealed by a new purification procedure and EPR spectroscopy. J. Biol. Chem. 272, 23206–23210.
[9] Liu, W., Kamensky, Y., Kakkar, R., Foley, E., Kulmacz, R.J. and Palmer, G. (2005) Purification and characterization of bovine adrenal cytochrome b561 expressed in insect and yeast cell systems. Protein Expr. Purif. 40, 429–439.
[10] Takeuchi, F., Hori, H., Obayashi, E., Shiro, Y. and Tsubaki, M. (2004) Properties of two distinct centers of cytochrome b561 from bovine chromaffin vesicles studied by EPR, resonance Raman and ascorbate reduction assay. J. Biochem. 135, 53–64.
[11] Kamensky, Y., Liu, W., Tsai, A.-L., Kulmacz, R.J. and Palmer, G. (2007) Axial ligation and stoichiometry of heme centers in adrenal cytochrome b561. Biochemistry 46, 8647–8658.
[12] Liu, W., Rogge, C.E., da Silva, G.F.Z., Shinkarev, V.P., Tsai, A.-L., Kamensky, Y., Palmer, G. and Kulmacz, R.J. (2008) His92 and His110 selectively affect different heme centers of adrenal cytochrome b561. Biochim. Biophys. Acta 1777, 1218–1228.
[13] Bérczi, A., Desmet, F., Van Doorslaer, S. and Asard, H. (2010) Spectral characterization of the recombinant mouse tumor suppressor 101F6 protein. Eur. Biophys. J. 39, 1129–1142.
[14] Bérczi, A. and Asard, H. (2006) Characterization of an ascorbate-reducible cytochrome *b*561 by site-directed mutagenesis. Acta Biol. Szeged. 50, 55–59.
[15] Bérczi, A., Su, D., Lakshminarasimhan, M., Vargas, A.S. and Asard, H. (2005) Heterologous expression and site-directed mutagenesis of an ascorbate-reducible cytochrome b561. Arch. Biochem. Biophys. 443, 82–92.
[16] Henry, E.R. and Hofrichter, J. (1992) Singular value decomposition – application to analysis of experimental data. Methods Enzymol. 210, 129–192.
[17] Stoll, S. and Schweiger, A. (2006) EasySpin, a comprehensive software package for spectral simulation and analysis in EPR. J. Magn. Reson. 178, 42–55.
[18] Takeuchi, F., Hori, H. and Tsubaki, M. (2005) Selective perturbation of the intravesicular heme center of cytochrome b561 by cysteinyl modification with 4, 4-dithiodipyridine. J. Biochem. 138, 751–762.
[19] Kincaid, J.R. (2000) Theoretical and physical characterization (Kadish, K.M., Smith, K.M. and Guilard, R., Eds.), The Porphyrin Handbook, vol. 7, pp. 225–289, Academic Press, New York, NY.
[20] Hu, S., Smith, K.M. and Spiro, T.G. (1996) Assignment of protoheme resonance Raman spectra by heme labeling in myoglobin. J. Am. Chem. Soc. 118, 12638–12646.
[21] Choi, S., Spiro, T.G., Langny, K.C., Smith, K.M., Budd, D.L. and La Mar, G.N. (1982) Structural correlations and vinyl influences in resonance Raman spectra of protoheme complexes and proteins. J. Am. Chem. Soc. 104, 4345–4351.